CdSe Quantum Dots for Two-Photon Fluorescence Thermal Imaging

ARTICLE *in* NANO LETTERS · NOVEMBER 2010

Impact Factor: 13.59 · DOI: 10.1021/nl1036098 · Source: PubMed

NANO LETTERS

pubs.acs.org/NanoLett

CdSe Quantum Dots for Two-Photon Fluorescence Thermal Imaging

Laura Martinez Maestro,[†] Emma Martín Rodríguez,[†] Francisco Sanz Rodríguez,[‡] M. C. Iglesias-de la Cruz,[‡] Angeles Juarranz,[‡] Rafik Naccache,[||] Fiorenzo Vetrone,[§] Daniel Jaque,[†] John A. Capobianco,*[,||] and José García Solé*[,†]

[†]Fluorescence Imaging Group, Departamento de Física de Materiales, C-IV, Universidad Autónoma de Madrid, C/Francisco Tomás y Valiente 7, Madrid 28049, Spain, [‡]Departamento de Biología, Universidad Autónoma de Madrid, Madrid 28049, Spain, [§]Institut National de la Recherche Scientifique - Énergie, Matériaux et Télécommunications, Université du Québec, Varennes, QC J3X 1S2, Canada, and [||]Department of Chemistry and Biochemistry, Concordia University, 7141 Sherbrooke Street W, Montreal, QC H4B 1R6, Canada

ABSTRACT The technological development of quantum dots has ushered in a new era in fluorescence bioimaging, which was propelled with the advent of novel multiphoton fluorescence microscopes. Here, the potential use of CdSe quantum dots has been evaluated as fluorescent nanothermometers for two-photon fluorescence microscopy. In addition to the enhancement in spatial resolution inherent to any multiphoton excitation processes, two-photon (near-infrared) excitation leads to a temperature sensitivity of the emission intensity much higher than that achieved under one-photon (visible) excitation. The peak emission wavelength is also temperature sensitive, providing an additional approach for thermal imaging, which is particularly interesting for systems where nanoparticles are not homogeneously dispersed. On the basis of these superior thermal sensitivity properties of the two-photon excited fluorescence, we have demonstrated the ability of CdSe quantum dots to image a temperature gradient artificially created in a biocompatible fluid (phosphate-buffered saline) and also their ability to measure an intracellular temperature increase externally induced in a single living cell.

KEYWORDS Nanothermometry, two-photon microscopy, quantum dots, HeLa cancer cell, thermal sensing, fluorescence imaging

Thermal sensing at the micro- and nanoscales is required for high spatial resolution of temperature gradients and is an indispensible tool for dynamical studies of diverse small systems including electrical, photonic, and biological ones. Nanotechnology is providing fascinating approaches to solve this requirement by means of using nanothermal probes whose properties display a strong dependence on the local temperature.[1] In these "nanothermometers", the thermal sensing method relies upon the particular parameter that displays a temperature dependence, which gives rise to high resolution thermal imaging techniques, such as scanning thermal and molecular fluorescence polarization microscopies.[2−8]

Fluorescent materials are particularly relevant in nanothermometry since they operate as "non-contact" thermometers and can provide the dual function of imaging and temperature sensing at the nanoscale.[9] These multimodal nanothermometers constitute an excellent tool to investigate fluid systems and particularly biomedical systems, as the nanoprobes can be homogeneously dispersed in the entire medium with minimal interaction.[10] Fluorescent nanothermometers are based on the temperature dependence of the fluorescence features (intensity, band shape, peak position, Stokes shift, or lifetime). In this respect, organic dyes were the first exogenous multimodal fluorescent "molecular probes" used for imaging as well as measuring the temperature of single living cells.[11] However, organic probes are easily damaged with the ultraviolet−visible excitation light (photobleaching).[12] Thus, novel fluorescent probes were developed, which are based on nanoscale inorganic materials (nanoparticles) and are resistant to photobleaching while showing high thermal sensitivity.[13−22] With the commercial availability of femtosecond (fs) lasers, these nanoprobes were shown to produce significant emitted light under near-infrared (NIR) two-photon excitation, that is, after almost simultaneous absorption of two excitation photons.[23−26] The recent development of two-photon fluorescent microscopes has spurred research on two-photon excitation nanoparticles since they provide a much better spectral and spatial resolution than the traditional one-photon microscopes.[27]

Quantum dots (hereafter QDs) are by far the most used fluorescent nanoprobes for fluorescence imaging.[28,29] This is essentially due to well-known materials engineering methods to synthesize semiconductor nanocrystals with the desired QD size and homogeneous size distribution. This allows for the selection of the most convenient emitted color by means of size confinement. Moreover, the surface of these QDs can be suitably engineered to be monodispersible in fluids as well as to target specific cells like, for instance, a cancer cell, while having a relatively good biocompatibility.[30] An additional advantage is that they can be efficiently two-photon excited

* To whom correspondence should be addressed.
Received for review: 10/15/2010
Published on Web: 11/09/2010

DOI: 10.1021/nl1036098 | *Nano Lett.* **2010,** *10,* 5109–5115

in the NIR to produce visible luminescence.[26] Indeed, all these advantages have led to the commercialization of QD biolabels at the present time. Furthermore, it has been previously reported that the intensity and peak wavelength of the QDs are influenced by the environmental temperature, thus giving rise to the opportunity of using them as fluorescent nanoprobes for fluorescence thermal imaging.[16,17,31−35] However, the reported images were acquired by means of one-photon excitation and thus, present limited applicability to high-resolution experiments (like temperature gradients) and particularly, to biomedical imaging, where multiphoton excitation is essential.

In this work, we have evaluated the ability of CdSe-QDs to act as fluorescent nanothermometers to realize thermal imaging by means of the modern multiphoton fluorescence-imaging microscopes. We have initially evaluated the fluorescence response of CdSe-QDs for thermal detection under both one-photon and two-photon excitation by systematically recording their emission spectra as a function of temperature in the physiological temperature range. The different excitation methods lead to diverse thermal behaviors and the fluorescence parameters that can be used for thermal sensing have been determined and calibrated. Once the CdSe-QDs have been fully characterized as two-photon excited fluorescent thermal nanoprobes, they have been used to determine the thermal gradients induced in a liquid by a focused laser beam. Finally, we demonstrate the potential of these two-photon excited nanothermometers in biomedical imaging by measuring the temperature evolution of a single HeLa cancer cell. To the best of our knowledge, these constitute the first two-photon excited thermal images obtained using CdSe-QDs.

CdSe spherical nanoparticles of 4 nm in diameter from Invitrogen Inc. (Qtracker 655) were dispersed in phosphate buffered saline (PBS) at a concentration of 0.3 μM. The solution was placed in an open oven so that its temperature could be varied in the physiological range between 30 to 70 °C with an accuracy of 1 °C. One-photon excitation was achieved by using a continuous wave air cooled Argon laser (Spectra Physics 177-G02, 488 nm, and 10 mW output power). This wavelength lies just below the absorption edge (not included for the sake of brevity) of the CdSe-QDs/PBS solution thus ensuring one-photon excitation. Moreover, we verified that this absorption edge is almost temperature independent and so no differences should be expected in the temperature dependence of the emission when using different one-photon excitation wavelengths. In fact, we examined this by exciting at 377 nm (pulsed N_2 laser) and it led to the same results as for 488 nm excitation. As two-photon fluorescence microscopes make use of fs-pulsed excitation laser sources, we used a mode-locked Ti:Sapphire laser (Spectra Physics Tsunami, 100 fs pulse duration, 80 MHz repetition rate, and 100 mW output power) for two-photon excitation, which was set at 800 nm, the wavelength peak in the two-photon excitation spectrum (not shown). Both excitation beams were focused into the solution containing the QDs by using a 10× optical microscope objective.

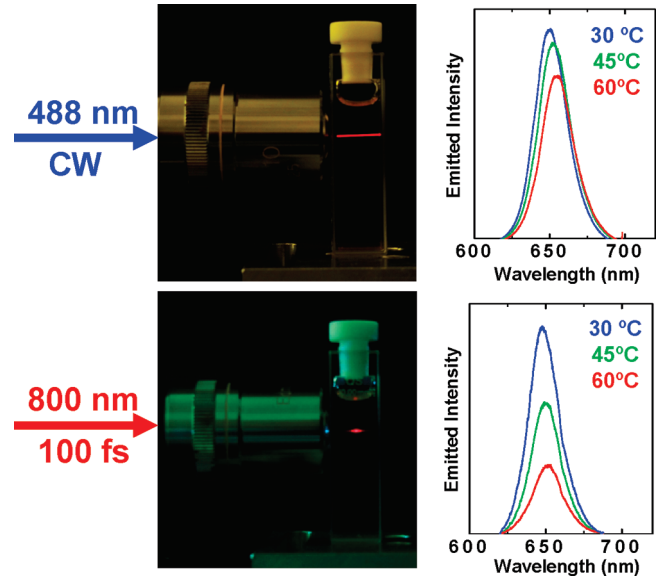

FIGURE 1. (Left side) Digital images of the CdSe-QDs/PBS solution obtained at room temperature under one-photon (top) and two-photon (bottom) optical excitation, respectively. (Right side) Emission spectra of the CdSe-QDs/PBS solution at three different temperatures (30, 45, and 60 °C) as obtained under one-photon (top) and two-photon (bottom) excitation, respectively.

Figure 1 (left side) presents digital images of the CdSe-QDs/PBS solution obtained at room temperature under both one-photon and two-photon excitation. It can be clearly seen that the active fluorescent volume is reduced by two-photon illumination, as this excitation becomes efficient only at the focus of the illumination beam (where the highest photon densities are achieved) and leads to a higher confinement of the fluorescence with respect to one-photon excitation. This higher confinement allows for the achievement of higher spatial resolutions (below the illuminating wavelength) that is required for the imaging of micro- and nanosystems.[27] Moreover, two-photon excitation allows for the generation of visible luminescence under NIR illumination, offering additional advantages for bioimaging applications, such as minimization of autofluorescence, increase of penetration depths and reduction of laser induced tissue damage.[36−38] Thus, a significant improvement in contrast and spatial resolution of the obtained thermal images would be achieved under two-photon NIR excitation of the CdSe-QDs.

Figure 1 (right side) also shows the emission spectra of the CdSe-QDs/PBS solution at three different temperatures (30, 45, and 60 °C) as obtained under both one-photon and two-photon excitation. It is clear that in both cases the peak fluorescence wavelength and the integrated emitted intensity are strongly influenced by temperature. Independent of the excitation mechanism, a temperature increase causes a red shift and, simultaneously, a reduction in the optical conversion efficiency (more remarkable under two-photon

DOI: 10.1021/nl1036098 | *Nano Lett.* **2010,** *10,* 5109–5115

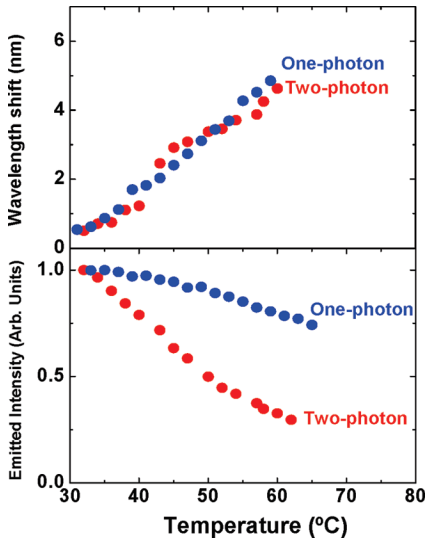

FIGURE 2. Temperature variation of the peak emission wavelength (top) and integrated emitted intensity (bottom) as obtained from the CdSe-QDs/PBS solution under one and two-photon excitation.

excitation). The simultaneous existence of these two temperature dependent fluorescence parameters allows for CdSe-QDs to be used as "dual thermal sensors" capable of temperature measurements by two complementary methods. As will be shown below, this fact allows for thermal imaging in systems with nonhomogeneous particle distributions (such as living cells).

For thermal imaging applications, an accurate calibration of the spectral features that will be used as thermal indicators is required. For this purpose, the integrated emitted intensity and peak wavelength have been systematically investigated as a function of temperature (shown in Figure 2). As can be observed, the thermally induced spectral red shift has been found to be, within experimental uncertainty, independent of the number of photons involved during excitation. In both one-photon and two-photon experiments, the peak emission wavelength variation as a function of temperature essentially followed a linear relationship. Thus, from a linear fit we have estimated a variation coefficient of 0.16 nm/°C, which is comparable to previously reported values in different QDs (ranging from 0.08 to 0.2 nm/°C).[17,34,35] This temperature-related shift obeys a variety of phenomena, including the thermally induced variation of the bandgap energy of the QDs, quantum yield of the emitting levels, thermal expansion of the QDs as well as the thermally induced variation of the solvent's refractive index.[34,39,40] The relative contribution of each phenomenon has been previously estimated in the case of CdSe-QDs, concluding that the thermally induced variation of the bandgap energy is the dominant one.[34] Thus, it is expected that the observed thermally induced spectral shift will be independent of the particular character of the excitation process, as observed in Figure 2a.

At variance with the thermally induced spectral shift, the reduction of the fluorescence efficiency as a function of temperature has been found to follow different trends for one-photon and two-photon excitations (see Figure 2b). For one-photon excitation, the fluorescence suffers only a moderate reduction (25% reduction for a temperature increment of 30 °C), whereas for two-photon excitation this reduction is three times larger (75% for the same temperature increment). According to previous studies, the temperature-induced decrease of the one-photon excited QD emission can be attributed to the thermal activation of surface trap states as well as to a thermally-induced increase in the nonradiative exciton recombination probability.[41,42] Following this argument we can estimate, from the one-photon excitation data, that the fluorescence quantum efficiency (Φ_f) of CdSe-QDs is reduced by a factor of 0.25 when the temperature is increased from 30 to 60 °C. The thermally induced reduction of the two-photon excited emission intensity requires a different analysis. This emission intensity (I_2) is proportional to the product of the two-photon absorption cross section (σ_2) and the fluorescence quantum efficiency, so that $I_2 \propto \Phi_f \cdot \sigma_2$.[26,43] The temperature dependence of the two-photon excited emission is, therefore, determined by thermally induced variations of both the fluorescence quantum efficiency and the two-photon absorption cross section. From the data obtained under one-photon excitation, we have estimated a 25% reduction of the fluorescence quantum efficiency, which is almost a third of the net reduction observed in the two-photon excited emission intensity. This fact suggests that the two-photon absorption cross section in CdSe-QDs is also strongly temperature dependent, playing in fact a dominant role in the two-photon excited fluorescence quenching. Independently of the dominant mechanism for thermal quenching of the two-photon excited emission, its behavior is of great relevance for thermal imaging purposes since it leads to a much higher thermal sensitivity than for one-photon excitation. Thus, this enhanced thermal sensitivity together with the enhanced spatial resolution of two-photon excited fluorescence make these CdSe-QDs nanoprobes particularly suitable for high-resolution nanothermometry.

After we investigated the temperature influence on the two-photon excited emission features of the CdSe-QDs/PBS solution, the next step was to demonstrate its use for two-photon fluorescence thermal imaging. For this purpose, we have performed imaging experiments in two different fluid systems.

First, by means of a pump−probe experiment we have artificially created a light-induced thermal gradient in our solution and this gradient has been properly imaged by using the temperature dependence of the CdSe-QD emission intensity (Figure 2b). A continuous wave 980 nm laser beam (the pump) was focused into the solution. This is partially absorbed by the PBS solvent but not by the QDs and the absorbed energy is subsequently delivered as heat. As the absorption profile is not homogeneous, greater heating is expected at the focus compared to the surrounding area, thus a temperature gradient should be created in the solu-

DOI: 10.1021/nl1036098 | *Nano Lett.* **2010,** *10,* 5109–5115

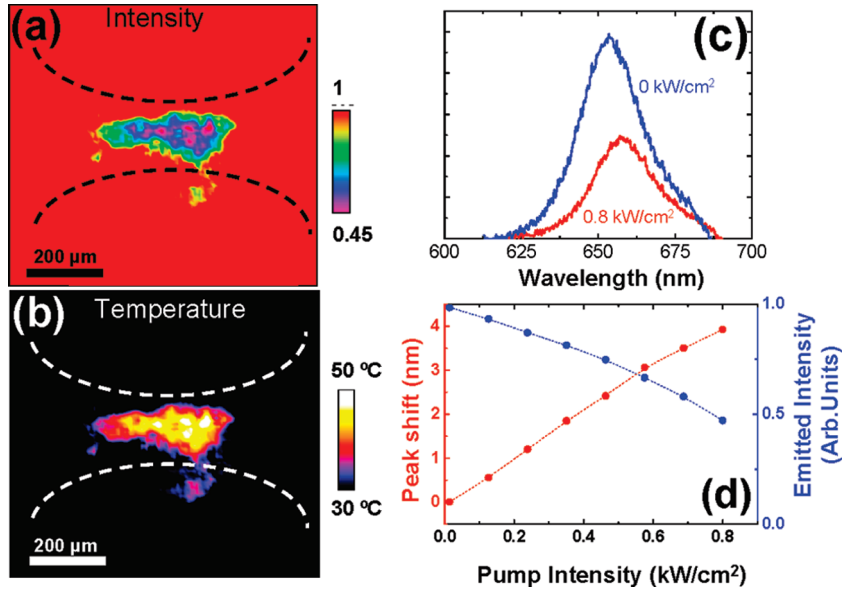

FIGURE 3. (a) Spatial variation of the two-photon excited emission intensity as obtained from a CdSe-QDs/PBS solution in the presence of a focused 980 nm heating laser beam (its profile schematically drawn with the dashed lines). (b) Thermal image of the CdSe-QDs/PBS solution denoting the local temperature increment at the 980 nm beam focus. (c) Emission spectra from a CdSe-QDs/PBS solution at focus for two different intensities of the pump (heating) beam. (d) Plots of the emission peak shift and emission intensity versus pump beam intensity at the focus of this heating beam.

tion. This gradient is imaged using two-photon fluorescence microscopy of the QDs, which are resonantly excited by an orthogonal probe laser beam.

The 980 nm laser pump beam was focused down to a spot size of 200 μm. Under these conditions the maximum density achieved in the PBS solution was estimated to be lower than 0.8 kW/cm^2. For such low intensities the density fluctuations due to optical forces can be neglected and thus we can consider that the spatial distribution of the QDs within the solution is homogeneous. This aspect makes it possible to use the emitted intensity of the QDs to image the created thermal gradient. For this purpose, the locally heated CdSe-QDs/PBS solution was incorporated into a fiber-coupled confocal microscope. The luminescence of the CdSe-QDs was then two-photon excited by means of a 100 fs, 800 nm excitation beam (the probe) focused into the solution orthogonally to the 980 nm pump beam. The probe beam was focused with a 10× microscope objective, which was also used to collect the 650 nm generated luminescence of the CdSe-QDs. The Numerical Aperture of the 10× microscope objective was 0.25 from which we have estimated a spatial (lateral) resolution close to 2.5 μm. After passing through confocal apertures, the two-photon excited luminescence was analyzed by means of a fiber coupled high resolution spectrometer. The XY motorized stage on which the solution was mounted allowed us to scan the 800 nm probe beam in the surroundings of the 980 nm pump focal point. Figure 3a shows the spatial variation of the two-photon excited emission intensity. In this image, the dotted black lines schematically represent the 980 nm beam path. As it can be observed, the emitted intensity is strongly reduced at focus. According to the data of Figure 2, this can be attributed to the achievement of higher temperatures at focus (as it was indeed expected). The data presented in Figure 2b allows for the calibration of this intensity image in terms of temperature variations. Thus, the corresponding thermal gradient image is presented in Figure 3b and demonstrates that the temperature at focus has been raised by almost 20 °C. Because of the large integration times required in our experimental setup for the acquisition of the two-photon excited spectra with low signal-to-noise ratio (above 10 s per spectrum), the acquisition of thermal images based on the temperature induced spectral shifts was not possible. Nevertheless, it should be noted that thermal measurement of fluids cannot be only obtained through the temperature-induced luminescence quenching of QDs but also from their temperature-induced spectral shift. To account for this, the emission spectra generated at the focus of the heating beam were measured for different 980 nm heating beam intensities. In Figure 3c, we have included the two-photon emission spectra generated for two different pump intensities. It is clear that when the 980 nm beam intensity is increased both an emission intensity decrease and a spectral shift to longer wavelengths are simultaneously induced. Figure 3d shows the induced spectral peak shift and luminescence quenching as a function of the pump beam intensity. For the largest pump intensity used in this work, a maximum spectral shift of 3.9 nm and a relative intensity reduction of 52% have been found. Thus, the maximum temperature increment induced at focus has been found to be close to 24 °C, when calculated based on the spectral shift, and 20 °C, when calculated from the observed emission intensity reduction. Therefore, the discrepancy between these two alternative methods has been found to be ±2 °C,

DOI: 10.1021/nl1036098 | *Nano Lett.* **2010,** *10,* 5109–5115

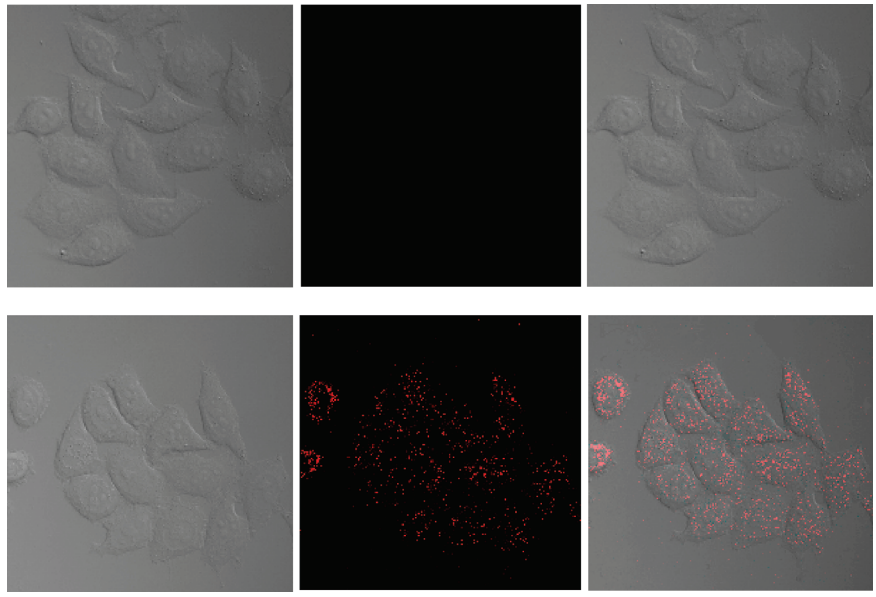

FIGURE 4. Room-temperature optical transmission images of HeLa cells nonincubated (top figures) and incubated with the CdSe-QDs/PBS solution (bottom figures). (Left side) Images taken with the optical transmission microscope incorporated in the multiphoton fluorescence setup. (Middle) Two-photon excited fluorescence images. (Right side) Superimposed (fluorescence and optical transmission) images.

that is, less than 10% of the measured value. The origin of this discrepancy could arise from the density fluctuation that can be generated in the fluid due to the local heating. Thus, the ability of CdSe-QDs to image thermal gradients of locally heated liquids by two-photon excited fluorescence microscopy is clearly demonstrated.

The CdSe-QDs were subsequently incorporated in HeLa cervical cancer cells in order to investigate their thermometric ability in biological systems. For this purpose, immortalized human carcinoma cells were incubated for 2 h with the CdSe-QD nanothermometers (using the solution from Figure 1) and imaged by two-photon fluorescence microscopy. To confirm the successful internalization of the QDs into the cancer cells they were imaged with a fast multiphoton microscope (Zeiss LSM510 microscope), so that the images of several cells could be obtained. Figure 4 shows the optical transmission image (left column), the fluorescence image (middle column), and the superimposed images (right column) of a group of HeLa cancer cells incubated in the absence (top row) and presence (bottom row) of QDs. Excitation and collection wavelengths were 800 and 650 nm, respectively. These images put into evidence a full incorporation of the QDs into the cancer cells as it has also been observed for targeted gold nanorods.[44] This was further confirmed by the measurement of the cross-sectional multiphoton excited fluorescence images of single cancer cells as well as by the analysis of the emission spectra generated when the NIR laser was focused inside and outside the cell. Moreover, it has been found that the multiphoton excited emission spectrum generated from the cell well matched that obtained from the original QDs solutions (see Figure 1). Thus, any possible contribution of autofluorescence to the images in Figure 4 must be discarded. When the NIR excitation beam was focused outside the cancer cells no fluorescence signal was observed. It is also clearly observed that the CdSe-QDs have been internalized by the HeLa cells but their distribution inside these cells is inhomogeneous. Thus, in this particular case it is more appropriate to measure cell internal temperature changes by means of the spectral shift of the CdSe-QDs emission. At first glance it was observed that the peak shift was essentially constant within the cell area where the nanoparticles were incorporated in a sufficient concentration to be detected by two-photon fluorescence imaging. This fact indicated that the temperature was essentially constant (25 °C) throughout the entire cell. Thus, to evaluate the ability of the CdSe-QDs for detecting cell temperature changes, the cell temperature was externally varied by using a microair-heater so that the cells could be externally heated, as schematically shown in Figure 5 (left side). The intracellular temperature increase due to the hot air flow caused a clear change in the two-photon excited emission of the QDs incorporated inside the cell. This can be clearly observed when the emission spectrum was recorded at heating times of 0 and 3 min (top right side in Figure 5). In these experiments, the 800 nm excitation beam was focused inside the cell by means of a 100× microscope objective with a Numerical Aperture of 0.9 (giving a lateral spatial resolution close to 400 nm). Intracellular heating was evidenced by a clear red shift of the QDs emission band. By recording the two-photon excited emission for different heating times and using the calibration graph of Figure 2, we were able to measure intracellular temperature in real time. Results are shown in Figure 5 (bottom right side), which shows the intracel-

DOI: 10.1021/nl1036098 | *Nano Lett.* **2010,** *10,* 5109–5115

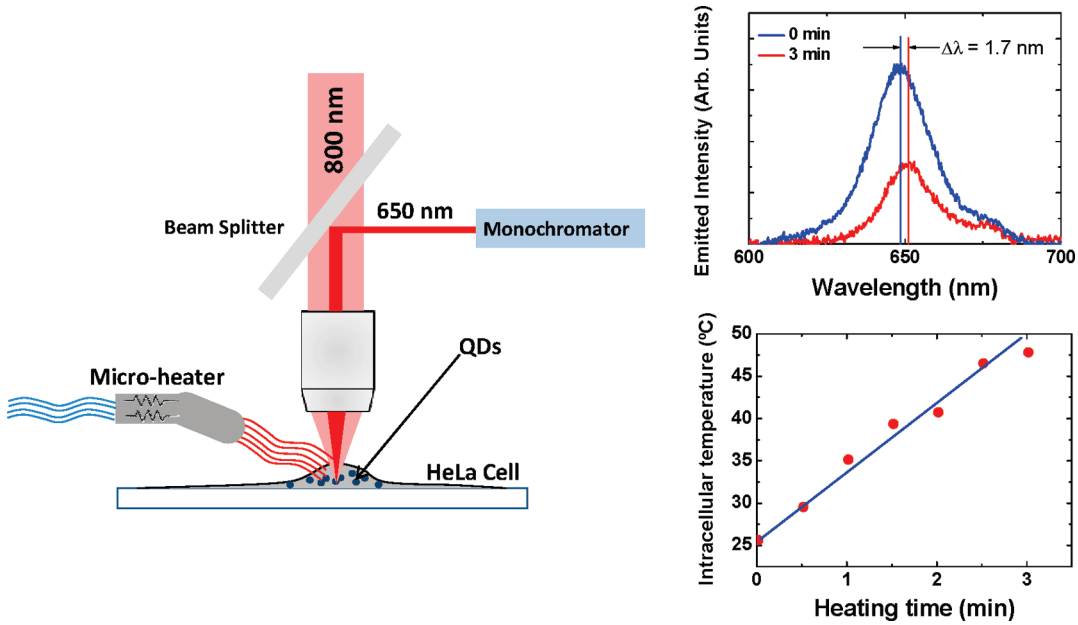

FIGURE 5. (Left side) Schematic diagram of the experimental setup used to monitor intracellular heating through two-photon CdSe-QDs fluorescence thermometry. (Right side) Two-photon fluorescence spectra generated by the CdSe-QDs incorporated in a HeLa cell for two different heating temperatures (top). Graph at bottom shows the intracellular temperature as calculated from the spectral shift of the CdSe-QDs two-photon emission as obtained for different heating times.

lular temperature measured by the CdSe-QDs nanothermometers as a function of heating time. Indeed, it is clearly demonstrated that a temperature increase of about 25 °C (from 25 to about 50 °C) can be precisely determined by the two-photon excited emission shift of the nanothermometers. During this temperature interval the cell shape remained essentially unchanged. Because of the experimental configuration, temperatures higher than 50 °C lead to a distortion of the fluid cell system and the results are not reliable. Nevertheless, these results demonstrate for the first time the ability of the CdSe-QDs as nanothermometers for two-photon fluorescence bioimaging.

In summary, we have demonstrated that CdSe-QDs constitute multifunctional thermal probes for nanothermometry of fluid systems. On one hand, these QDs present two fluorescence features (emission peak and intensity) dependent on the environment temperature. On the other hand, they can be imaged by means of the novel high-resolution two-photon fluorescence microscopes. In addition, it has been found that for thermal imaging purposes luminescence obtained through two-photon excitation has relevant advantages over the traditional one-photon excitation. First, two-photon excitation leads to a larger spatial resolution due to its nonlinear nature. Second, the higher temperature sensitivity of the emitted light obtained under two-photon excitation leads to higher quality thermal images. These properties have enabled us to record a high quality thermal gradient image in a fluid (PBS) and to measure internal temperature changes of a single HeLa cell. To the best of our knowledge, these are the first results of QDs used as nanothermometers for high-resolution two-photon fluorescence thermal imaging. The results reported here open a new avenue of possibilities in the nanothermometry of fluids if these well-known optical probes are used.

Acknowledgment. This work was supported by the Universidad Autónoma de Madrid and Comunidad Autonoma de Madrid (Projects CCG087-UAM/MAT-4434 and S2009/MAT- 1756), by the Spanish Ministerio de Educacion y Ciencia (MAT 2007−64686 and MAT2010-16161), and by a Banco Santander-CEAL-UAM project. The authors also thank the Natural Sciences and Engineering Research Council (NSERC) of Canada and the Gouvernement du Québec, Ministère du Développement économique, de l'Innovation et de l'Exportation for funding. J.G.S. thanks the Spanish Minsterio de Educación for financial support for a research stay at Concordia University (ref PR2009−0040). Authors also thank the technicians of the multi-photon microscope for their help and assistance during the experiments.

Note Added after ASAP Publication. The author list was incomplete in the version of this paper published November 9, 2010. The correct version published November 11, 2010.

REFERENCES AND NOTES

(1) Lee, J.; Kotov, N. A. *Nano Today* **2007**, *2*, 48–51.
(2) Dorozhkin, P. S.; Tovstonog, S. V.; Golberg, D.; Zhan, J.; Ishikawa, Y.; Shiozawa, M.; Nakanishi, H.; Nakata, K.; Bando, Y. *Small* **2005**, *1*, 1088–1093.
(3) Gao, Y.; Bando, Y. *Nature* **2002**, *415*, 599.
(4) Lan, Y.; Wang, H.; Chen, X.; Wang, D.; Chen, G.; Ren, Z. *Adv. Mater.* **2009**, *21*, 4839–4844.
(5) Lee, J.; Govorov, A. O.; Kotov, N. A. *Angew. Chem.* **2005**, *117*, 7605–7608.
(6) Engeser, M.; Fabbrizzi, L.; Licchelli, M.; Sacchi, D. *Chem. Commun.* **1999**, *1999*, 1191–1192.
(7) Majumdar, A. *Ann. Rev. Mat. Sci.* **1999**, *29*, 505–585.

DOI: 10.1021/nl1036098 | *Nano Lett.* **2010,** *10,* 5109–5115

(8) Zondervan, R.; Kulzer, F.; van der Meer, H.; Disselhorst, J. A. J. M.; Orrit, M. *Biophys. J.* **2006**, *90*, 2958–2969.
(9) Wang, S.; Westcott, S.; Chen, W. *J. Phys. Chem. B* **2002**, *106*, 11203–11209.
(10) Ohulchanskyy, T. Y.; Roy, I.; Yong, K.-T.; Pudavar, H. E.; Prasad, P. N. *Wiley Interdiscip. Rev.: Nanomed. Nanobiotechnol.* **2010**, *2*, 162–175.
(11) Chapman, C. F.; Liu, Y.; Sonek, G. J.; Tromberg, B. J. *Photochem. Photobiol.* **1995**, *62*, 416–425.
(12) Song, L.; Hennink, E. J.; Young, T.; Tanke, H. J. *Biophys. J.* **1995**, *68*, 2588–2600.
(13) Medintz, I. L.; Uyeda, T. H.; Goldman, E. R.; Mattoussi, H. *Nat. Mater.* **2005**, *4*, 435–446.
(14) Wang, H.; Huff, T. B.; Zweifel, D. A.; Wei, He; Low, P. S.; Wei, A.; Cheng, J.-X. *Proc. Natl. Acad. Sci. U.S.A.* **2005**, *102*, 15752–15756.
(15) Huang, X.; El-Sayed, I. H.; Qian, W.; El-Sayed, M. A. *J. Am. Chem. Soc.* **2006**, *128*, 2115–2120.
(16) Jorge, P. A. S.; Mayeh, M.; Benrashid, R.; Caldas, P.; Santos, J. L.; Farahi., F. *Meas. Sci. Technol.* **2006**, *17*, 1032–1038.
(17) Walker, G. W.; Sundar, V. C.; Rudzinski, C. M.; Wun, A. W.; Bawendi, M. G.; Nocera, D. G. *Appl. Phys. Lett.* **2003**, *83*, 3555–3557.
(18) Vetrone, F.; Naccache, R.; Zamarron, A.; Juarranz de la Fuente, A.; Sanz-Rodriguez, F.; Martinez Maestro, L.; Martin Rodriguez, E.; Jaque, D.; Garcia Sole, J.; Capobianco, J. A. *ACS Nano* **2010**, *4*, 3254–3258.
(19) Aigouy, L.; Tessier, G.; Mortier, M.; Charlot, B. *Appl. Phys. Lett.* **2005**, *87*, 184105-1–184105-3.
(20) Saïdi, E.; Samson, B.; Aigouy, L.; Volz, S.; Löw, P.; Bergaud, C.; Mortier, M. *Nanotechnology.* **2009**, *20*, 115703/1–115703/8.
(21) Allison, S. W.; Gillies, G. T.; Rondinone, A. J.; Cates, M. R. *Nanotechnology* **2003**, *14*, 859–863.
(22) Wade, S. A.; Collins, S. F.; Baxter, G. W. *J. Appl. Phys.* **2003**, *94*, 4743–4756.
(23) Hilderbrand, S. A.; Shao, F.; Salthouse, C.; Mahmood, U.; Weissleder, R. *Chem. Commun.* **2009**, 4188–4190.
(24) Yi, G.; Lu, H.; Zhao, S.; Ge, Y.; Yang, W.; Chen, D.; Guo, L.-H. *Nano Lett.* **2004**, *4*, 2191–2196.
(25) Kang, H.; Jia, B.; Li, J.; Morrish, D.; Gu, M. *Appl. Phys. Lett.* **2010**, *96*, No. 063702.
(26) Larson, D. R.; Zipfel, W. R.; Williams, R. M.; Clark, S. W.; Bruchez, M. P.; Wise, F. W. *Science* **2003**, *300*, 1434–1436.
(27) Xu, C.; Zipfel, W.; Shear, J. B.; Williams, R. M.; Webb, W. W. *Proc. Natl. Acad. Sci. U.S.A.* **1996**, *93*, 10763–10768.
(28) Michalet, X.; Pinaud, F. F.; Bentolila, L. A.; Tsay, J. M.; Doose, S.; Li, J. J.; Sundaresan, G.; Wu, A. M.; Gambhir, S. S.; Weiss, S. *Science* **2005**, *307*, 538–544.
(29) Chan, W. C. W.; Nie, S. *Science* **1998**, *281*, 2016–2018.
(30) Derfus, A. M.; Chan, W. C. W.; Bhatia, S. N. *Nano Lett.* **2004**, *4*, 11–18.
(31) Wei Liu, J.; Zhang, Y.; Ge, C. W.; Jin, Y. L.; Hu, S. L.; Gu, N. *Chin. Chem. Lett.* **2009**, *20*, 977–980.
(32) Kim, J. C.; Rho, H.; Smith, L. M.; Jackson, H. E.; Lee, S.; Dobrowolska, M.; Furdyna, J. K. *Appl. Phys. Lett.* **1999**, *75*, 214–216.
(33) Han, B.; Hanson, W. L.; Bensalah, K.; Tuncel, A.; Stern, J. M.; Cadeddu, J. A. *Ann. Biomed. Eng.* **2009**, *37*, 1230–1239.
(34) Yu, H. C. Y.; Leon-Saval, S. G.; Argyros, A.; Barton, G. W. *Appl. Opt.* **2010**, *49*, 2749–2752.
(35) Li, S.; Zhang, K.; Yang, J.-M.; Lin, L.; Yang, H. *Nano Lett.* **2007**, *7*, 3102–3105.
(36) König, K. *J. Microsc. (Oxford, U.K.)* **2000**, *200*, 83–104.
(37) Venugopalan, V.; Nishioka, N. S.; Mikic, B. B. *Biophys. J.* **1996**, *70*, 2981–2993.
(38) So, M. K.; Xu, C. J.; Loening, A. M.; Gambhir, S. S.; Rao, J. H. *Nat. Biotechnol.* **2006**, *24*, 339–343.
(39) Liu, T. C.; Huang, Z. L.; Wang, H. Q.; Wang, J. H.; Li, X. Q.; Zhao, Y. D.; Luo, Q. M. *Analyt. Chim. Acta.* **2006**, *559*, 120–123.
(40) Leistikow, M. D.; Johansen, J.; Kettelarij, A. J.; Lodahl, P.; Vos, W. L. *Phys. Rev. B.* **2009**, *79*, No. 045301.
(41) Biju, V.; Makita, Y.; Sonoda, A.; Yokoyama, H.; Baba, Y.; Ishikawa, M. *J. Phys. Chem. B.* **2005**, *109*, 13899–13905.
(42) Nomura, S.; Kobayashi, T. *Phys. Rev. B.* **1992**, *45*, 1305–1316.
(43) He, G. S.; Yong, K.-T.; Zheng, Q.; Sahoo, Y.; Baev, A.; Ryasnyanskiy, A. I.; Prasad, P. N. *Opt. Express* **2007**, *15*, 12818–12833.
(44) Durr, N. J.; Larson, T; Smith, D. K.; Korgel, B. A.; Sokolov, K.; Ben-Yakar, A. *Nano Lett.* **2007**, *7*, 941–945.

DOI: 10.1021/nl1036098 | *Nano Lett.* **2010,** *10,* 5109–-5115